Complex Frequency Divider

Ignacio Ponce, Federico Milano
School of Electrical & Electronic Engineering, University College Dublin (UCD), Ireland
ignacio.poncearancibia@ucdconnect.ie, federico.milano@ucd.ie

***Abstract*—This work presents the Complex Frequency Divider Formula (CFDF), an explicit equation for the complex frequencies (CFs) of the voltage of every bus of a power system in terms of a linear combination of the CFs of the currents injected by the devices connected to the network. The coefficients of this linear combination depend on the topology of the system, voltages and currents. The CFDF carries valuable information on the impact of every device on the dynamic of the voltage and frequency of any particular bus of the system. The formulation is exact, as it does not require any simplification of the dynamic model of the system. The CFDF is implemented in two benchmark systems to show its potential in static and dynamic analysis in different scenarios. Finally, relevant notes on the applications of the proposed formula are outlined.**

***Index Terms*—Complex frequency, frequency divider, frequency estimation, low-inertia systems, power system dynamics.**

I. Introduction

A. Motivation

The ongoing move towards renewable, distributed, and converter-interfaced generation is leading to deep changes in the dynamic behavior of power systems. A well-recognized immediate consequence of these changes is the need to develop new tools for the modeling, control and stability analysis of modern power systems [1]–[5]. In this vein, the concept of *complex frequency* (CF) has been recently presented in [6] to give a more general and precise definition of the frequency, unifying the relationship between the variations of the device's current injections and the voltage and frequency dynamics at a particular bus. In [6], the CF is obtained as a function of power variations through implicit equations, where the CF of the voltage of a bus is written in terms of the current injected at the bus and the neighbor voltage CF. It remains an open and relevant question how to relate explicitly the CF of the voltage of a bus with the current injections of all the devices connected to the network. The objective of this work is to determine such a relationship.

B. Literature Review

There is a growing interest in using the CF as it is showing promising applications, see, for example, [7]–[11]. These references show that a precise evaluation of the CF can significantly improve the monitoring, modeling and control of the system. It is, of course, possible to estimate it through PMUs, PLLs or numerical approximations of the derivatives. However, these approaches are vulnerable to noise and unbalances [12] and perform poorly after disturbances [13].

Analytical methods avoid aforementioned issues at a cost of increasing mathematical and computational complexity. For example, reference [14] proposes a method for calculating the frequency at load buses for time-domain simulations. However, the approach utilised in [14] is not general as it requires a specific structure of the dynamic model of synchronous machines and loads.

Another example of analytical method is the Frequency Divider Formula (FDF) that provides the frequency at every bus of the network in terms of the angular speed of all the synchronous machines [15]. However, the FDF requires several simplifications, e.g. neglecting voltage magnitude variations and assumes that the only devices able to modify bus frequencies are the synchronous machines. Following works have focused on extending the FDF to consider the effect of other devices. For example, the inertia contribution of DFIG generators is included in [16] based on Thevenin equivalents. An extension of the FDF to include the effect of the frequency control capability of Inverter-Based Resources (IBRs) is presented in [17], where converter controllers are formulated to resemble the structure of synchronous machines, thus allowing their inclusion in the FDF. In both cases, the estimation given by the extended FDF still requires simplifications and is device-model dependent. In this work we propose a technique that overcomes the intrinsic structural limits of the FDF and extends it to the complex domain.

C. Contributions

The contributions of the paper are as follows:

- The formulation of the Complex Frequency Divider Formula (CFDF), that is, an explicit expression for the CF of the voltage of every bus as a linear function of the CF of the current injected by every device. This formulation is general, systematic and model-agnostic.
- An analytical solution for the CF using the proposed formula. This solution requires the knowledge of the device's dynamic models. The structure required covers the vast majority of device models.
- Specific expressions for the CF of the current injected by commonly used device models. These expressions are required for the analytical solution presented.

D. Paper Organization

The remainder of this paper is organized as follows. Section II presents the proposed CFDF. An analytical solution for

This work is supported by the Sustainable Energy Authority of Ireland (SEAI) by funding I. Ponce and F. Milano under project FRESLIPS, Grant No. RDD/00681.

a range of common dynamic devices is also presented, and specific expressions for basic models are provided. The implementation of the proposed formulation in two study cases is described in Section III. Relevant remarks on the applications of the proposed CFDF are also included in Section III. Finally, Section IV presents the conclusions and outlines future work.

II. Complex Frequency Divider Formula

A. Derivation

Consider a system with n buses. The starting point is the current balance equations at network buses:

$$\bar{\boldsymbol{i}} = \bar{\boldsymbol{Y}}\,\bar{\boldsymbol{v}}\,, \tag{1}$$

where $\bar{\boldsymbol{i}}, \bar{\boldsymbol{v}} \in \mathbb{C}^{n\times 1}$ are column vectors containing the net current injections and the voltage at every bus, respectively; and $\bar{\boldsymbol{Y}} \in \mathbb{C}^{n\times n}$ is the admittance matrix of the system, which is assumed to be constant, i.e., transmission system dynamics are neglected. This simplification is adopted exclusively for simplicity. However, line dynamics can be incorporated by treating them as time-varying admittances with their corresponding complex frequency. The interested reader can find an example of this in [18].

Recalling the property of the CF to act as a linear derivative operator of Park vectors [6], one can define the CFs of the voltage vector ($\bar{\boldsymbol{\eta}}$) and the current injection vector ($\bar{\boldsymbol{\xi}}$) as follows:

$$\begin{aligned} \dot{\bar{\boldsymbol{v}}} &= \mathrm{diag}(\bar{\boldsymbol{v}})\,\bar{\boldsymbol{\eta}}\,, \\ \dot{\bar{\boldsymbol{i}}} &= \mathrm{diag}(\bar{\boldsymbol{i}})\,\bar{\boldsymbol{\xi}}\,, \end{aligned} \tag{2}$$

where $\mathrm{diag}(\bar{\boldsymbol{v}}), \mathrm{diag}(\bar{\boldsymbol{i}}) \in \mathbb{C}^{n\times n}$ are diagonal matrices which elements are the bus voltages and current injections, respectively. Differentiating (1) with respect to time and isolating the CF of the voltage leads to the proposed CFDF:

$$\boxed{\bar{\boldsymbol{\eta}} = \bar{\boldsymbol{D}}\,\bar{\boldsymbol{\xi}}} \tag{3}$$

where $\bar{\boldsymbol{\eta}}, \bar{\boldsymbol{\xi}} \in \mathbb{C}^{n\times 1}$ are column vectors containing the complex frequency of voltages and net current injections at every bus, respectively, and:

$$\begin{aligned} \bar{\boldsymbol{D}} &= [\bar{\boldsymbol{Y}}\mathrm{diag}(\bar{\boldsymbol{v}})]^{-1}\mathrm{diag}(\bar{\boldsymbol{i}}) \\ &= \mathrm{diag}(\bar{\boldsymbol{v}})^{-1}\bar{\boldsymbol{Y}}^{-1}\mathrm{diag}(\bar{\boldsymbol{i}}) \\ &= \mathrm{diag}(\bar{\boldsymbol{v}})^{-1}\bar{\boldsymbol{Z}}\mathrm{diag}(\bar{\boldsymbol{i}})\,. \end{aligned} \tag{4}$$

where $\bar{\boldsymbol{Z}} = \bar{\boldsymbol{Y}}^{-1}$ is the (dense) impedance matrix of the grid. Note that we have assumed that the voltages and currents are differentiable.

The matrix $\bar{\boldsymbol{D}}$ is composed of dimensionless complex numbers which depend on the topology, voltages and currents injected into the transmission system. Note that the value of the (h,k) element of $\bar{\boldsymbol{D}}$, say $\bar{D}_{hk}$, can be seen as a coefficient representing the participation of the CF of the net current injected of a device connected at bus k to the CF of the voltage at bus h. In particular, the real part represents the impact of the frequency of the current on ω_h (imaginary part of the CF of the voltage), and the impact of the rate of change of the magnitude of the current on ρ_h (real part of the CF of the voltage). Also, the imaginary part measures the cross-participation, i.e., the impact of the frequency of the current on ρ_h, and the effect of the current magnitude rate of change on ω_h.

The elements of the $\bar{\boldsymbol{D}}$ matrix provide information on the participation of a device to the CF of every network bus. These elements embed information on the topology (as they are built using the network admittance matrix) and grid operating conditions (as they are obtained for a given power flow solution). However, note that the actual participation of a device also depends on its specific dynamic response and control. For instance, for an arbitrary bus h, a synchronous machine connected at bus k can have a lower participation than a constant impedance load connected at bus j, that $\bar{D}_{hk} < \bar{D}_{hj}$, due to their locations and current injected to the grid. However, the actual impact of the synchronous machine dynamics to the frequency of the system is certainly higher than that of the impedance, which is a passive device.

Another interesting property holds for the matrix $\bar{\boldsymbol{D}}$: each row coefficients are naturally normalized, i.e., the real part of each row of sums 1, and the imaginary part sums 0 (the proof can be found in Appendix). Summarizing, for every bus of the power system, $\bar{\boldsymbol{D}}$ informs through dimensionless and naturally normalized coefficients, the participation of every device dynamic, taking into account both: the topology (transmission system model), and the operating conditions (voltages and currents injections).

B. Explicit Expressions of Bus Voltage Frequencies

Equation (3) can be used in time-domain simulations to calculate the frequency of the voltage at every bus of the grid. While PLL measurements can be used for a model-agnostic calculation of the CFDF, it is relevant to note that (3) can also serve to find *analytic* and *explicit* expressions for $\bar{\boldsymbol{\eta}}$. The procedure we propose in this paper consists in formulating $\bar{\boldsymbol{\xi}}$ in terms of system states and algebraic variables. Depending on the dynamic model of the devices of the system, $\bar{\boldsymbol{\xi}}$ can be also a function of $\bar{\boldsymbol{\eta}}$, in which case, (3) becomes an *implicit* equation. The ability to find an explicit solution for $\bar{\boldsymbol{\eta}}$ depends on the shape of $\bar{\boldsymbol{\xi}}(\bar{\boldsymbol{\eta}}, \boldsymbol{x}, \boldsymbol{y})$, where $\boldsymbol{x} \in \mathbb{R}^{n_x\times 1}, \boldsymbol{y} \in \mathbb{R}^{n_y\times 1}$ are column vectors containing the existing n_x system states and n_y algebraic variables, respectively.

For the analytical derivation of the expression of $\bar{\boldsymbol{\eta}}$, we proceed as follows. First, observe that $\bar{\boldsymbol{\xi}}$ can be written in general as:

$$\bar{\boldsymbol{\xi}}(\bar{\boldsymbol{\eta}}, \boldsymbol{x}, \boldsymbol{y}) = \bar{\boldsymbol{\xi}}_{\mathrm{a}}(\boldsymbol{x}, \boldsymbol{y}) + \bar{\boldsymbol{\xi}}_{\mathrm{p}}(\bar{\boldsymbol{\eta}}, \boldsymbol{x}, \boldsymbol{y})\,, \tag{5}$$

where $\bar{\boldsymbol{\xi}}_{\mathrm{a}}$ is the $\bar{\boldsymbol{\eta}}$-independent part of devices $\bar{\boldsymbol{\xi}}$, and $\bar{\boldsymbol{\xi}}_{\mathrm{p}}$ is the $\bar{\boldsymbol{\eta}}$-dependent part. While $\bar{\boldsymbol{\xi}}_{\mathrm{a}}$ is known and defined in terms of the variables of the system, $\bar{\boldsymbol{\xi}}_{\mathrm{p}}$ depends on $\bar{\boldsymbol{\eta}}$ thus making (3) implicit. In the following, we derive the solution for the case $\bar{\boldsymbol{\xi}}_{\mathrm{p}}$ dependency on $\bar{\boldsymbol{\eta}}$ can be written as:

$$\bar{\boldsymbol{\xi}}_{\mathrm{p}}(\bar{\boldsymbol{\eta}}, \boldsymbol{x}, \boldsymbol{y}) = \bar{\boldsymbol{\kappa}}_{\rho}(\boldsymbol{x}, \boldsymbol{y})\,\boldsymbol{\rho} + \bar{\boldsymbol{\kappa}}_{\omega}(\boldsymbol{x}, \boldsymbol{y})\,\boldsymbol{\omega}\,, \tag{6}$$

where $\bar{\boldsymbol{\kappa}}_{\rho}, \bar{\boldsymbol{\kappa}}_{\omega} \in \mathbb{C}^{n\times n}$ are matrices containing complex functions of existing system variables, and $\boldsymbol{\rho}, \boldsymbol{\omega} \in \mathbb{R}^{n\times 1}$ are

column vectors containing the real and imaginary parts of $\bar{\boldsymbol{\eta}}$, respectively. Equation (6) holds in general as $\bar{\boldsymbol{\xi}}$ is obtained as the point differentiation of the current injections of the devices. The examples given in Section II-C show how to determine (6) explicitly for a variety of common power system dynamic device models.

Next, the derivation of $\bar{\boldsymbol{\eta}}$ expressions begins by replacing (5) and (6) in (3):

$$\begin{aligned}\bar{\boldsymbol{\eta}} &= \bar{\boldsymbol{D}}\,\bar{\boldsymbol{\xi}} \\ &= \bar{\boldsymbol{D}}\,(\bar{\boldsymbol{\xi}}_{\mathrm{a}} + \bar{\boldsymbol{\xi}}_{\mathrm{p}}) \\ &= \bar{\boldsymbol{D}}\,\bar{\boldsymbol{\xi}}_{\mathrm{a}} + \bar{\boldsymbol{D}}\,(\bar{\boldsymbol{\kappa}}_{\rho}\,\boldsymbol{\rho} + \bar{\boldsymbol{\kappa}}_{\omega}\,\boldsymbol{\omega})\,.\end{aligned} \tag{7}$$

Then, taking the real and imaginary parts of (7):

$$\boldsymbol{\rho} = \Re\left\{\bar{\boldsymbol{D}}\,\bar{\boldsymbol{\xi}}_{\mathrm{a}}\right\} + \Re\left\{\bar{\boldsymbol{D}}\,\bar{\boldsymbol{\kappa}}_{\rho}\right\}\,\boldsymbol{\rho} + \Re\left\{\bar{\boldsymbol{D}}\,\bar{\boldsymbol{\kappa}}_{\omega}\right\}\,\boldsymbol{\omega}\,, \tag{8}$$

$$\boldsymbol{\omega} = \Im\left\{\bar{\boldsymbol{D}}\,\bar{\boldsymbol{\xi}}_{\mathrm{a}}\right\} + \Im\left\{\bar{\boldsymbol{D}}\,\bar{\boldsymbol{\kappa}}_{\rho}\right\}\,\boldsymbol{\rho} + \Im\left\{\bar{\boldsymbol{D}}\,\bar{\boldsymbol{\kappa}}_{\omega}\right\}\,\boldsymbol{\omega}\,, \tag{9}$$

and extracting $\boldsymbol{\rho}$ from (8):

$$\boxed{\boldsymbol{\rho} = \boldsymbol{C}_1\left(\Re\left\{\bar{\boldsymbol{D}}\,\bar{\boldsymbol{\xi}}_{\mathrm{a}}\right\} + \Re\left\{\bar{\boldsymbol{D}}\,\bar{\boldsymbol{\kappa}}_{\omega}\right\}\,\boldsymbol{\omega}\right)} \tag{10}$$

where $\boldsymbol{C}_1 = (\mathbb{I}_n - \Re\left\{\bar{\boldsymbol{D}}\,\bar{\boldsymbol{\kappa}}_{\rho}\right\})^{-1}$ and $\mathbb{I}_n \in \mathbb{R}^{n\times n}$ is the identity matrix. Replacing (10) in (9) yields:

$$\boldsymbol{C}_2\,\boldsymbol{\omega} = \Im\left\{\bar{\boldsymbol{D}}\,\bar{\boldsymbol{\xi}}_{\mathrm{a}}\right\} + \Im\left\{\bar{\boldsymbol{D}}\,\bar{\boldsymbol{\kappa}}_{\rho}\right\}\,\boldsymbol{C}_1\,\Re\left\{\bar{\boldsymbol{D}}\,\bar{\boldsymbol{\xi}}_{\mathrm{a}}\right\}\,, \tag{11}$$

where

$$\boldsymbol{C}_2 = \mathbb{I}_n - \Im\left\{\bar{\boldsymbol{D}}\,\bar{\boldsymbol{\kappa}}_{\omega}\right\} - \Im\left\{\bar{\boldsymbol{D}}\,\bar{\boldsymbol{\kappa}}_{\rho}\right\}\,\boldsymbol{C}_1\,\Re\left\{\bar{\boldsymbol{D}}\,\bar{\boldsymbol{\kappa}}_{\omega}\right\}\,. \tag{12}$$

Next, extracting $\boldsymbol{\omega}$:

$$\boldsymbol{\omega} = {\boldsymbol{C}_2}^{-1}\left(\Im\left\{\bar{\boldsymbol{D}}\,\bar{\boldsymbol{\xi}}_{\mathrm{a}}\right\} + \Im\left\{\bar{\boldsymbol{D}}\,\bar{\boldsymbol{\kappa}}_{\rho}\right\}\,\boldsymbol{C}_1\,\Re\left\{\bar{\boldsymbol{D}}\,\bar{\boldsymbol{\xi}}_{\mathrm{a}}\right\}\right). \tag{13}$$

or, equivalently:

$$\boxed{\boldsymbol{\omega} = \boldsymbol{D}_{\mathrm{re}}\,\Re\left\{\bar{\boldsymbol{\xi}}_{\mathrm{a}}\right\} + \boldsymbol{D}_{\mathrm{im}}\,\Im\left\{\bar{\boldsymbol{\xi}}_{\mathrm{a}}\right\}} \tag{14}$$

where

$$\boldsymbol{D}_{\mathrm{re}} = {\boldsymbol{C}_2}^{-1}\left(\Im\left\{\bar{\boldsymbol{D}}\right\} + \Im\left\{\bar{\boldsymbol{D}}\,\bar{\boldsymbol{\kappa}}_{\rho}\right\}\,\boldsymbol{C}_1\,\Re\left\{\bar{\boldsymbol{D}}\right\}\right), \tag{15}$$

$$\boldsymbol{D}_{\mathrm{im}} = {\boldsymbol{C}_2}^{-1}\left(\Re\left\{\bar{\boldsymbol{D}}\right\} - \Im\left\{\bar{\boldsymbol{D}}\,\bar{\boldsymbol{\kappa}}_{\rho}\right\}\,\boldsymbol{C}_1\,\Im\left\{\bar{\boldsymbol{D}}\right\}\right). \tag{16}$$

Equations (10) and (14) are the sought analytic expressions of $\bar{\boldsymbol{\eta}}$. In particular, (14) is an explicit formula for the frequencies at every bus that depends only on the $\bar{\boldsymbol{\eta}}$-independent part of the device's dynamics. Thus, the problem reduces to find $\bar{\boldsymbol{\xi}}_a$, $\bar{\boldsymbol{\kappa}}_{\rho}$ and $\bar{\boldsymbol{\kappa}}_{\omega}$, which depend on the dynamic model used for every device of the power system. Specific expressions for common device models are provided in the following subsection.

C. Power System's Device Models

Expressions for $\bar{\boldsymbol{\xi}}_a$, $\bar{\boldsymbol{\kappa}}_{\rho}$ and $\bar{\boldsymbol{\kappa}}_{\omega}$ are provided in this section for specific dynamic models of common devices in a power system.

1) 4th-order Synchronous Machines: Consider the well-known 4th-order two axes dynamic model of synchronous machines in the dq-frame [19], where symbols have the usual meanings:

$$\dot{\delta} = \Omega_{\mathrm{b}}(\omega - 1)\,, \tag{17}$$

$$M\dot{\omega} = \tau_{\mathrm{m}} - \tau_{\mathrm{e}} - D(\omega - 1)\,, \tag{18}$$

$$T'_{\mathrm{d0}}\dot{e}'_{\mathrm{q}} = v_{\mathrm{f}} - (X_{\mathrm{d}} - X'_{\mathrm{d}})\imath_{\mathrm{d}} - e'_{\mathrm{q}}\,, \tag{19}$$

$$T'_{\mathrm{q0}}\dot{e}'_{\mathrm{d}} = (X_{\mathrm{q}} - X'_{\mathrm{q}})\imath_{\mathrm{q}} - e'_{\mathrm{d}}\,, \tag{20}$$

along with the algebraic equations:

$$\bar{v} = v_{\mathrm{d}} + \jmath\, v_{\mathrm{q}} = v\sin(\delta - \theta) + jv\cos(\delta - \theta)\,, \tag{21}$$

$$\bar{\imath} = \imath_{\mathrm{d}} + \jmath\,\imath_{\mathrm{q}} = \imath\sin(\delta - \beta) + \imath\cos(\delta - \beta)\,, \tag{22}$$

$$\bar{s} = p + \jmath\, q = (v_{\mathrm{d}}\imath_{\mathrm{d}} + v_{\mathrm{q}}\imath_{\mathrm{q}}) + \jmath(v_{\mathrm{q}}\imath_{\mathrm{d}} - v_{\mathrm{d}}\imath_{\mathrm{q}})\,, \tag{23}$$

$$\tau_{\mathrm{e}} = \psi_{\mathrm{q}}\imath_{\mathrm{d}} - \psi_{\mathrm{d}}\imath_{\mathrm{q}}\,, \tag{24}$$

$$\bar{\psi} = \psi_{\mathrm{d}} + \jmath\psi_{\mathrm{q}} = (e'_{\mathrm{q}} - X'_{\mathrm{d}}\imath_{\mathrm{d}}) - \jmath(e'_{\mathrm{d}} + X'_{\mathrm{q}}\imath_{\mathrm{q}})\,, \tag{25}$$

$$\bar{v} = -R_{\mathrm{s}}\bar{\imath} - \jmath\,\bar{\psi}\,. \tag{26}$$

First we note that applying the time derivative to the grid interface algebraic equations (21)-(22), using (17), and denoting the rotor speed as $\omega_{\mathrm{r}} = \Omega_{\mathrm{b}}\omega$, we get:

$$\dot{v}_{\mathrm{d}} = \rho v_{\mathrm{d}} - \omega v_{\mathrm{q}} + v_{\mathrm{q}}\omega_{\mathrm{r}}\,, \tag{27}$$

$$\dot{v}_{\mathrm{q}} = \rho v_{\mathrm{q}} + \omega v_{\mathrm{d}} - v_{\mathrm{d}}\omega_{\mathrm{r}}\,, \tag{28}$$

$$i_{\mathrm{d}} = \Re\left\{\bar{\xi}\right\}\imath_{\mathrm{d}} - \Im\left\{\bar{\xi}\right\}\imath_{\mathrm{q}} + \imath_{\mathrm{q}}\omega_{\mathrm{r}}\,, \tag{29}$$

$$i_{\mathrm{q}} = \Re\left\{\bar{\xi}\right\}\imath_{\mathrm{q}} + \Im\left\{\bar{\xi}\right\}\imath_{\mathrm{d}} - \imath_{\mathrm{d}}\omega_{\mathrm{r}}\,, \tag{30}$$

which, extracting the CF of the stator current, can be conveniently rewritten as:

$$\bar{\xi} = \left(\frac{\imath_{\mathrm{d}}i_{\mathrm{d}} + \imath_{\mathrm{q}}i_{\mathrm{q}}}{i^2}\right) + \jmath\left(\frac{\imath_{\mathrm{d}}i_{\mathrm{q}} - \imath_{\mathrm{q}}i_{\mathrm{d}}}{i^2} + \omega_{\mathrm{r}}\right), \tag{31}$$

We now obtain the expressions of i_{d} and i_{q} as functions of the state variables and $\bar{\eta}$. With this aim, derivating with respect to time the stator magnetic algebraic equations (25), one obtains:

$$i_{\mathrm{d}} + \jmath\, i_{\mathrm{q}} = \left(\frac{\dot{e}'_{\mathrm{q}}}{X'_{\mathrm{d}}} - \frac{\dot{\psi}_{\mathrm{d}}}{X'_{\mathrm{d}}}\right) - \jmath\left(\frac{\dot{e}'_{\mathrm{d}}}{X'_{\mathrm{q}}} + \frac{\dot{\psi}_{\mathrm{q}}}{X'_{\mathrm{q}}}\right), \tag{32}$$

which, using the expression of the stator fluxes obtained from (26), can be rewritten as:

$$i_{\mathrm{d}} + \jmath\, i_{\mathrm{q}} = \frac{\dot{e}'_{\mathrm{q}} - \dot{v}_{\mathrm{q}} - R_{\mathrm{s}}i_{\mathrm{q}}}{X'_{\mathrm{d}}} - \jmath\,\frac{\dot{e}'_{\mathrm{d}} - \dot{v}_{\mathrm{d}} - R_{\mathrm{s}}i_{\mathrm{d}}}{X'_{\mathrm{q}}}\,, \tag{33}$$

or, equivalently:

$$i_{\mathrm{d}} = \frac{X'_{\mathrm{q}}(\dot{e}'_{\mathrm{q}} - \dot{v}_{\mathrm{q}}) + R_{\mathrm{s}}(-\dot{e}'_{\mathrm{d}} + \dot{v}_{\mathrm{d}})}{X'_{\mathrm{d}}X'_{\mathrm{q}} - R_{\mathrm{s}}^2}\,, \tag{34}$$

$$i_{\mathrm{q}} = \frac{X'_{\mathrm{d}}(-\dot{e}'_{\mathrm{d}} + \dot{v}_{\mathrm{d}}) + R_{\mathrm{s}}(\dot{e}'_{\mathrm{q}} - \dot{v}_{\mathrm{q}})}{X'_{\mathrm{d}}X'_{\mathrm{q}} - R_{\mathrm{s}}^2}\,, \tag{35}$$

and, using (27) and (28), one can obtain the following final expressions for the time derivative of the current:

$$i_{\mathrm{d}} = \frac{\dot{e}'_{\mathrm{q}}}{X'_{\mathrm{d}}} - \frac{(\rho v_{\mathrm{q}} + \omega v_{\mathrm{d}} - \omega_{\mathrm{r}}v_{\mathrm{d}} + R_{\mathrm{s}}i_{\mathrm{q}})}{X'_{\mathrm{d}}}\,, \tag{36}$$

$$i_{\mathrm{q}} = -\frac{\dot{e}'_{\mathrm{d}}}{X'_{\mathrm{q}}} - \frac{(-\rho v_{\mathrm{d}} + \omega v_{\mathrm{q}} - \omega_{\mathrm{r}}v_{\mathrm{q}} - R_{\mathrm{s}}i_{\mathrm{d}})}{X'_{\mathrm{q}}}\,. \tag{37}$$

Then, substituting the expressions above for i_d and i_q into (31), we obtain the sougth expression of $\bar{\xi}$:

$$\boxed{\begin{aligned}\bar{\xi} = &\frac{\bar{\imath}^*(\bar{Z}_\mathrm{d}(v_\mathrm{q}\omega_\mathrm{r} - \dot{e}'_\mathrm{d}) + j\bar{Z}^*_\mathrm{q}(v_\mathrm{d}\omega_\mathrm{r} + \dot{e}'_\mathrm{q}))}{(X'_\mathrm{d}X'_\mathrm{q} - R_\mathrm{s}^2)\imath^2} \\ &+ \frac{\bar{\imath}^*(\bar{Z}_\mathrm{d}v_\mathrm{d} - \bar{Z}^*_\mathrm{q}jv_\mathrm{q})}{(X'_\mathrm{d}X'_\mathrm{q} - R_\mathrm{s}^2)\imath^2}\rho \\ &+ \jmath\left(\frac{-\bar{\imath}^*(\bar{Z}^*_\mathrm{q}v_\mathrm{d} - \bar{Z}_\mathrm{d}jv_\mathrm{q})}{(X'_\mathrm{d}X'_\mathrm{q} - R_\mathrm{s}^2)\imath^2}\omega + \omega_\mathrm{r}\right)\end{aligned}} \tag{38}$$

where $\dot{e}'_\mathrm{q}$ and $\dot{e}'_\mathrm{d}$ are defined by (19) and (20), and we have used the notation $\bar{Z}_\mathrm{d} = (R_\mathrm{s} + jX'_\mathrm{d})$ and $\bar{Z}_\mathrm{q} = (R_\mathrm{s} + jX'_\mathrm{q})$. Finally, the terms $\bar{\xi}_\mathrm{a}$, $\bar{\kappa}_\rho$ and $\bar{\kappa}_\omega$ of the 4th-order model of the synchronous machine are:

$$\begin{aligned}\bar{\xi}_\mathrm{a} &= j\omega_\mathrm{r} + \frac{\bar{\imath}^*(\bar{Z}_\mathrm{d}(v_\mathrm{q}\omega_\mathrm{r} - \dot{e}'_\mathrm{d}) + \jmath\bar{Z}^*_\mathrm{q}(v_\mathrm{d}\omega_\mathrm{r} + \dot{e}'_\mathrm{q}))}{(X'_\mathrm{d}X'_\mathrm{q} - R_\mathrm{s}^2)\imath^2}\,, \\ \bar{\kappa}_\rho &= \frac{\bar{\imath}^*(\bar{Z}_\mathrm{d}v_\mathrm{d} - \jmath\bar{Z}^*_\mathrm{q}v_\mathrm{q})}{(X'_\mathrm{d}X'_\mathrm{q} - R_\mathrm{s}^2)\imath^2}\,, \quad \bar{\kappa}_\omega = j\frac{\bar{\imath}^*(\jmath\bar{Z}_\mathrm{d}v_\mathrm{q} - \bar{Z}^*_\mathrm{q}v_\mathrm{d})}{(X'_\mathrm{d}X'_\mathrm{q} - R_\mathrm{s}^2)\imath^2}\,.\end{aligned} \tag{39}$$

For a second-order classical model of the machine, namely $R_\mathrm{s} = 0$, $X'_\mathrm{q} = X'_\mathrm{d}$, $T'_{\mathrm{d}0} = T'_{\mathrm{q}0} = 0$, and $v_\mathrm{f} = \text{const.}$, the expressions in (38) and (39) simplify as:

$$\bar{\xi} = \jmath\,\omega_\mathrm{r} + \frac{\bar{s}}{X'_d\imath^2}(\omega_\mathrm{r} + \jmath\,\bar{\eta})\,, \tag{40}$$

$$\bar{\xi}_\mathrm{a} = \jmath\omega_\mathrm{r} + \frac{\bar{s}\,\omega_\mathrm{r}}{X'_d\imath^2}\,, \quad \bar{\kappa}_\rho = \frac{\jmath\,\bar{s}}{X'_\mathrm{d}\imath^2}\,, \quad \bar{\kappa}_\omega = -\frac{\bar{s}}{X'_\mathrm{d}\imath^2}\,. \tag{41}$$

2) ZIP Loads: Consider a constant impedance load whose equations are as follows:

$$\bar{s} = \bar{s}_0\,\frac{v^2}{v_0^2}\,. \tag{42}$$

The time derivative of (42) gives:

$$\dot{\bar{s}} = 2\,\bar{s}_0\frac{v\,\dot{v}}{v_0^2} = 2\,\rho\,\bar{s}\,. \tag{43}$$

Recalling the following identity for the CF (see [7], Section III):

$$\dot{\bar{s}} = \bar{s}\,(\bar{\eta} + \bar{\xi}^*)\,, \tag{44}$$

and using (43) and (44), one has:

$$\bar{s}\,(\bar{\eta} + \bar{\xi}^*) = 2\,\rho\,\bar{s}\,. \tag{45}$$

From the latter expression, it descends that:

$$\boxed{\bar{\xi} = \bar{\eta}} \tag{46}$$

Finally, $\bar{\xi}_\mathrm{a}$, $\bar{\kappa}_\rho$ and $\bar{\kappa}_\omega$ are found for the z-load as:

$$\bar{\xi}_\mathrm{a} = 0\,, \qquad \bar{\kappa}_\rho = 1\,, \qquad \bar{\kappa}_\omega = \jmath\,. \tag{47}$$

Note that, as expected, this device is entirely $\bar{\boldsymbol{\eta}}$-dependent (passive). A similar procedure can be followed for different ZIP load models. For example, for a constant current load, one has:

$$\boxed{\bar{\xi} = \jmath\,\omega} \tag{48}$$

with

$$\bar{\xi}_\mathrm{a} = 0\,, \qquad \bar{\kappa}_\rho = 0\,, \qquad \bar{\kappa}_\omega = \jmath\,, \tag{49}$$

and for the constant power load:

$$\boxed{\bar{\xi} = -\bar{\eta}^*} \tag{50}$$

with

$$\bar{\xi}_\mathrm{a} = 0\,, \qquad \bar{\kappa}_\rho = -1\,, \qquad \bar{\kappa}_\omega = \jmath\,. \tag{51}$$

3) Inverter-Based Resources (IBR): Consider a simplified IBR converter model with active and reactive power control, ideal synchronization, and a droop frequency control. Using the usual notation for variables and parameters, the set of differential-algebraic equations are [20]:

$$T_\mathrm{d}\dot{\imath}_\mathrm{d} = \imath_\mathrm{dref} - \imath_\mathrm{d} = \Delta\imath_\mathrm{d}\,, \tag{52}$$

$$T_\mathrm{q}\dot{\imath}_\mathrm{q} = \imath_\mathrm{qref} - \imath_\mathrm{q} = \Delta\imath_\mathrm{q}\,, \tag{53}$$

$$T_\mathrm{f}\dot{x}_\mathrm{p} = -\frac{1}{R}(\omega_\mathrm{ref} - \omega) - x_\mathrm{p}\,, \tag{54}$$

$$p_\mathrm{ref} = p_{\mathrm{ref}0} + x_\mathrm{p}\,, \tag{55}$$

$$p_\mathrm{ref} + \jmath q_\mathrm{ref} = v_\mathrm{d}\imath_\mathrm{dref} + \jmath\,v_\mathrm{d}\imath_\mathrm{qref} \tag{56}$$

$$\imath_\mathrm{d} + \jmath\,\imath_\mathrm{q} = \imath\cos(\beta - \theta) + \jmath\,\imath\sin(\beta - \theta)\,, \tag{57}$$

where $\omega = \dot{\theta}$. Differentiating (57), the complex frequency of the current injected into the grid is:

$$\bar{\xi} = \left(\frac{\imath_\mathrm{d}\dot{\imath}_\mathrm{d} + \imath_\mathrm{q}\dot{\imath}_\mathrm{q}}{\imath^2}\right) + \jmath\left(\frac{\imath_\mathrm{d}\dot{\imath}_\mathrm{q} - \imath_\mathrm{q}\dot{\imath}_\mathrm{d}}{\imath^2} + \omega\right), \tag{58}$$

Then, replacing (52) and (53) in (58) leads to:

$$\Re\left\{\bar{\xi}\right\} = \frac{T_\mathrm{q}\imath_\mathrm{d}\Delta\imath_\mathrm{d} + T_\mathrm{d}\imath_\mathrm{q}\Delta\imath_\mathrm{q}}{T_\mathrm{d}T_\mathrm{q}\imath^2}\,, \tag{59}$$

$$\Im\left\{\bar{\xi}\right\} = \frac{T_\mathrm{d}\imath_\mathrm{d}\Delta\imath_\mathrm{q} - T_\mathrm{q}\imath_\mathrm{q}\Delta\imath_\mathrm{d}}{T_\mathrm{d}T_\mathrm{q}\imath^2} + \omega\,, \tag{60}$$

or, equivalently:

$$\boxed{\bar{\xi} = \frac{\bar{\imath}^*}{\imath^2}\left(\frac{\Delta\imath_\mathrm{d}}{T_\mathrm{d}} + \jmath\,\frac{\Delta\imath_\mathrm{q}}{T_\mathrm{q}}\right) + \jmath\,\omega} \tag{61}$$

and, hence, the terms $\bar{\xi}_\mathrm{a}$, $\bar{\kappa}_\rho$ and $\bar{\kappa}_\omega$ of the IBR are:

$$\bar{\xi}_\mathrm{a} = \frac{\bar{\imath}^*}{\imath^2}\left(\frac{\Delta\imath_\mathrm{d}}{T_\mathrm{d}} + \jmath\,\frac{\Delta\imath_\mathrm{q}}{T_\mathrm{q}}\right), \quad \bar{\kappa}_\rho = 0\,, \quad \bar{\kappa}_\omega = \jmath\,. \tag{62}$$

Finally, it is relevant to remark that all the derivations presented above hold and are sufficient to describe the device behavior even in case regulators are attached to them. For instance, turbine governors, AVRs, AGCs, additional outer loops in converters and any other controllers.

III. Case Studies

In this section, we apply the CFDF to the well-known IEEE 39 bus benchmark system, the single-line diagram of which is shown in Fig. 1. First, we examine the steady state values of the coefficients of $\bar{\boldsymbol{D}}$ for different buses, where we compare the potential influence of a device dynamic connected at different locations of the network. Then, we perform time-domain simulations to compare different methods to obtain

the frequency of the voltage. In particular, we compare our formula with the FDF and the frequency estimation obtained with a PLL. All simulations are obtained using the Python-based software tool Dome [21].

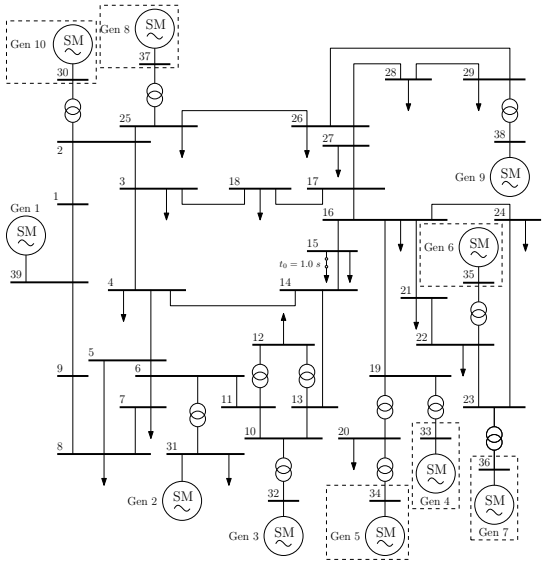

Fig. 1. Single-line diagram of the IEEE 39 bus benchmark system. Generators marked with the dashed rectangles are substituted with IBRs in the second scenario of the case study.

A. Quantification of Device Participation to the CF

The power flow solution of the system is used to compute the initial steady state values of $\bar{\boldsymbol{D}}$. We arbitrarily take buses 15 (load bus) and 35 (generator bus) to evaluate the coefficients. Devices are sorted according to the magnitude of their direct influence (real part of the coefficient). Those that mostly impact $\bar{\eta}$ are shown in Table I. Note that the devices that mostly participate to the frequencies of the selected buses are the devices that inject (draw) the highest powers to (from) the network. This suggests that rather than the specific location of the device, what mostly affects the value of the coefficients is the amount of power the device is exchanging with the grid. This effect is particularly evident in a compact and meshed network such as the New England 39-bus system.

As discussed in Section II-A, even though loads 39, 8 and 4 show high participation factors to the frequencies of buses 15 and 35, the impact on the frequency ultimately depends on the dynamic model and control of the devices connected to the grid. In the extreme case of being modeled as constant impedances, there is no independent internal variable at all as they are entirely passive devices. In such a case, the participation measured by $\bar{\boldsymbol{D}}$ spreads to the rest of the devices. As a consequence, the information provided by the elements of $\bar{\boldsymbol{D}}$ is especially useful for comparing the participation of devices of the same kind and size or with a similar dynamic model.

B. Calculation of the Frequency

We consider two scenarios. First, we apply the CFDF to the original IEEE 39 bus system, where a good performance of the FDF is expected since the system dynamic is dominated by synchronous generators, which are also well distributed throughout the grid. Then, we simulate a modified version of the system replacing some synchronous generators with IBRs. In both scenarios, a sudden disconnection of 200 MW and 96 MVAr at bus 15 is applied at $t_0 = 1.0$ s.

TABLE I
DEVICES THAT PARTICIPATE THE MOST TO $\bar{\eta}_{15}$ AND $\bar{\eta}_{35}$

Bus 15		Bus 35	
Device	Value	Device	Value
Load 39	0.314	Load 39	0.545
Gen 1	-0.274	Gen 1	-0.485
Load 8	0.212	Load 8	0.282
Load 4	0.201	Load 4	0.267
Gen 9	0.183	Gen 2	-0.173

1) Original IEEE 39 Bus System: The network is composed of ten synchronous generators. A 4th-order dynamic model as the one described in Section II-C1 is used for all the machines. A constant power model is used for all the loads. The transmission system is modeled through a constant admittance matrix. All the generators are equipped with Type 1 governors for primary frequency control and IEEE Type AC4 automatic voltage regulators. Finally, a standard automatic generation control provides secondary frequency regulation.

The frequency is evaluated at two different buses. First, at bus 15, where the load is suddenly disconnected. Second, at bus 35, a generator bus. For each case, we compare the frequency obtained through our formula, the FDF and a synchronous reference PLL. The results are shown in Figs. 2 and 3 for buses 15 and 35, respectively. As expected, the estimation given by the PLL experiences a numerical peak right after the event, especially in bus 15, from which the load is disconnected. After that, it gives a precise estimation of the frequency of the buses, thus serving as a reference for the analysis. Regarding the estimation given by the FDF, it is well-defined at every point of the simulation, as its dynamic is driven only by the state variable ω_r of the machines, which do not change discretely. However, the approximations on which the FDF is based lead to a deviation from the reference. This error is higher for buses far from synchronous machines (see, in this case, bus 15) than for those very close to them (bus 35). Finally, the calculation given by our formula outperforms the others, as it gives a precise result for the frequency without numerical issues.

For the sake of an example, Fig. 4 shows the frequency at bus 15 as obtained by solving the CFDF analytically and using the values of the CF of the current of every device as estimated with PLLs. Results verify that the PLL-based approximation is accurate except for the numerical issues right after the event.

2) Modified IEEE 39 Bus System: The IEEE 39 bus system is modified replacing 6 synchronous generators with IBRs, particularly, generators 4, 5, 6, 7, 8 and 10. The dynamic model described in Section II-C3 is used in all the IBRs. Thus, they have active and reactive power control, ideal synchronization, and a droop frequency control loop.

We consider buses 31 and 35 and show the results in Figs. 5 and 6, respectively. While the former is still connected to a synchronous machine bus, the latter is now connected to an IBR bus. The FDF performs reasonably well for the synchronous machine bus 31, and deviates from the exact value obtained with CFDF almost only in the magnitude of the oscillations. However, the deviation of the FDF with respect to the PLL and CFDF is higher for bus 35, as expected, as it cannot properly capture the shape of the local frequency deviations which are due to the IBR control. The results confirm the ability of the CFDF to accurately calculate the frequency at every bus independently of the type of devices connected to the grid and without numerical issues.

C. Remarks on the Applications of the CFDF

The matrix $\bar{\boldsymbol{D}}$ contains valuable information on how the dynamic of the devices participates to the dynamic of all the buses of the grid. However, the actual affectation of a specific internal variable of a device depends on its dynamic model, reflected in $\bar{\xi}$, not in $\bar{\boldsymbol{D}}$. Yet, the pure examination of the values of $\bar{\boldsymbol{D}}$ is appropriate for comparing the effect of devices of the same kind, or with a similar dynamic model. Moreover, since these coefficients have the properties of participation factors, they can be utilized to decide where to locate resources to support the control of $\bar{\boldsymbol{\eta}}$ at a specific bus or area of the grid.

The derivation of the CFDF does not require approximating the dynamic models of the devices connected to the grid. This feature implies that the CFDF, rather than a technique to estimate the CF of the voltage at every bus of the network, is in effect the actual analytic expression of the CF at the buses. We also note that, since the definition of the CFDF is based on differentiation of the differential-algebraic equations of the system, it is a linear (although time-variant) expression in terms of the CF. This makes possible to find the CF as an explicit function of the state and algebraic variables of the system.

Nevertheless, obtaining such expressions can be involved, as shown in Section II-C1 for the 4th-order synchronous machine model. The factorization of the dense matrix $\bar{\boldsymbol{D}}$ at every step of a time-domain simulation can also be cumbersome for large networks. Yet, an offline approach — i.e., solving (3) post-processing the results of the time-domain simulation — appears relevant if an exact value for $\bar{\boldsymbol{\eta}}$ is required. This can be used, for example, as a reference to compare the performance of different PLLs or other frequency estimators.

Finally, we note that (3) can also be evaluated by estimating $\bar{\boldsymbol{\xi}}$ through current measurements. This approach is accurate in practice, and as shown in the simulations of the case, except right after faults and events resulting in large sudden variations of bus voltages.

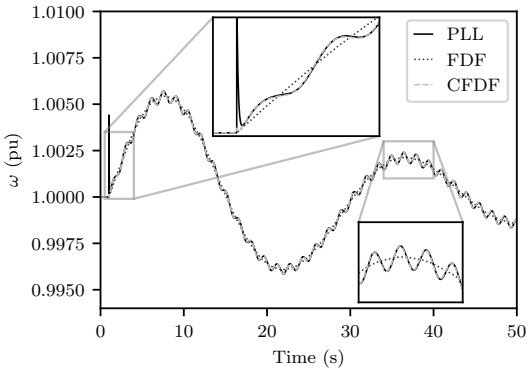

Fig. 2. Results for bus 15 - Original IEEE 39 bus system.

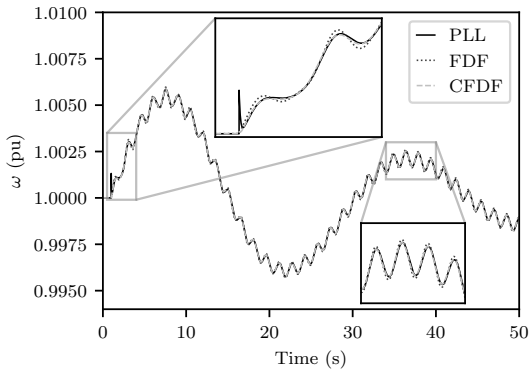

Fig. 3. Results for bus 35 - Original IEEE 39 bus system.

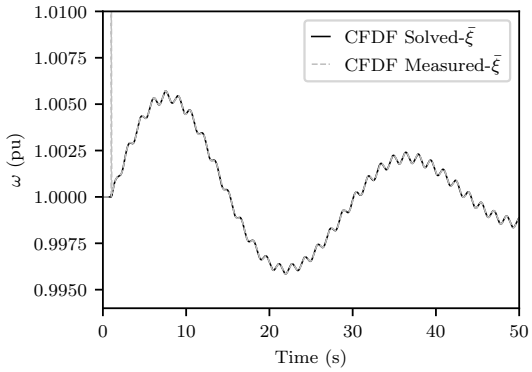

Fig. 4. Frequency at bus 15 calculated through the CFDF, analytical solution vs estimation.

IV. Conclusion

The paper introduces the CFDF, which is an explicit equation for the CF of the voltage of all buses ($\bar{\boldsymbol{\eta}}$) in terms of the CF of the current injected by the devices connected to the network ($\bar{\boldsymbol{\xi}}$). The paper shows how the coefficients of the matrix of the proposed formulation carry valuable information to quantify the participation of the different devices on the dynamic of $\bar{\boldsymbol{\eta}}$. The proposed formula can also be used to directly calculate $\bar{\boldsymbol{\eta}}$, either solving analytically or estimating $\bar{\boldsymbol{\xi}}$, for example, using PLLs.

The analytical solution is exact in the measure the dynamic model of the system is exact. It has a substantial theoretical value as it defines, explicitly, $\bar{\boldsymbol{\eta}}$ for every bus in terms of existing variables of the dynamic model. Therefore, it can

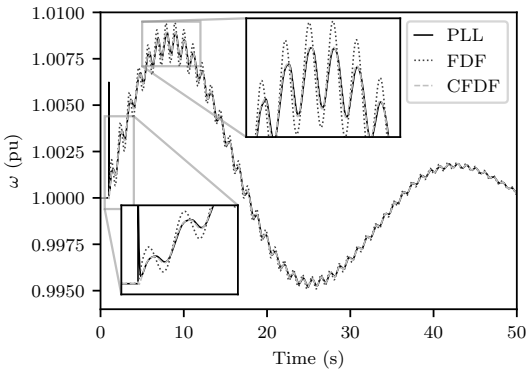

Fig. 5. Results for bus 31 - Modified IEEE 39 bus system.

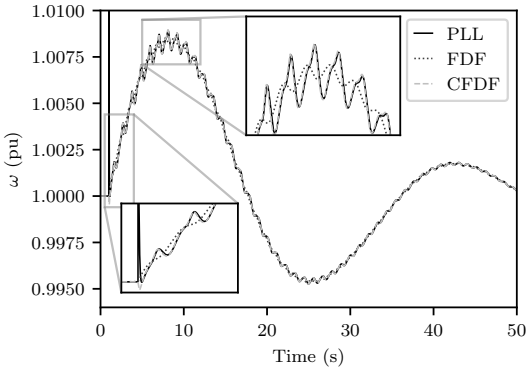

Fig. 6. Results for bus 35 - Modified IEEE 39 bus system.

serve as a reference to compare other methods to estimate the frequency at every bus. Nevertheless, its computational cost makes it more suitable for an offline analysis rather than integrating it into the set of DAEs of the system.

Future work will focus on reducing the computational cost of the CFDF. For example, by neglecting the terms corresponding to devices which, a priori are known to have a minor effect, or by solving the system only for a subset of buses of interest. Future research will also explore practical applications of the CFDF for control and dynamic state estimation.

APPENDIX

This appendix proves that the rows of $\bar{\boldsymbol{D}}$ always sum up 1. Equation (1) can be equivalently rewritten as:

$$\bar{\boldsymbol{Z}}\,\bar{\boldsymbol{i}} = \bar{\boldsymbol{v}}\,. \tag{63}$$

Then, consider the h-th row of equation (63):

$$\sum_{k=1}^{n} \bar{Z}_{hk}\bar{\imath}_k = \bar{v}_h \quad \Rightarrow \quad \frac{1}{\bar{v}_h}\sum_{k=1}^{n} \bar{Z}_{hk}\bar{\imath}_k = 1\,. \tag{64}$$

On the other hand, from (4), the (h,k)-element of $\bar{\boldsymbol{D}}$ is:

$$\bar{D}_{hk} = \frac{1}{\bar{v}_h}\bar{Z}_{hk}\bar{\imath}_k\,. \tag{65}$$

Taking the sum over the columns of $\bar{\boldsymbol{D}}$ for the h-th row:

$$\sum_{k=1}^{n} \bar{D}_{hk} = \frac{1}{\bar{v}_h}\sum_{k=1}^{n} \bar{Z}_{hk}\bar{\imath}_k\,, \tag{66}$$

and, recalling (64), one obtains:

$$\sum_{k=1}^{n} \bar{D}_{hk} = 1\,. \tag{67}$$

The proof is complete. □

REFERENCES

[1] N. Hatziargyriou *et al.*, "Definition and classification of power system stability – revisited & extended," *IEEE Transactions on Power Systems*, vol. 36, no. 4, pp. 3271–3281, 2021.

[2] F. Milano, F. Dörfler, G. Hug, D. J. Hill, and G. Verbič, "Foundations and challenges of low-inertia systems (invited paper)," in *2018 Power Systems Computation Conference (PSCC)*, 2018, pp. 1–25.

[3] M. N. H. Shazon, Nahid-Al-Masood, and A. Jawad, "Frequency control challenges and potential countermeasures in future low-inertia power systems: A review," *Energy Reports*, vol. 8, pp. 6191–6219, 2022.

[4] F. Dörfler and D. Groß, "Control of low-inertia power systems," *Annual Review of Control, Robotics, and Autonomous Systems*, vol. 6, pp. 415–445, 2023.

[5] IEEE Task Force on Modeling and Simulation of Large Power Systems with High Penetration of Inverter-Based Generation, "Simulation methods, models, and analysis techniques to represent the behavior of bulk power system connected inverter-based resources," IEEE, Tech. Rep., September 2023.

[6] F. Milano, "Complex frequency," *IEEE Transactions on Power Systems*, vol. 37, no. 2, pp. 1230–1240, 2022.

[7] D. Moutevelis, J. Roldán-Pérez, M. Prodanovic, and F. Milano, "Taxonomy of power converter control schemes based on the complex frequency concept," *arXiv preprint arXiv:2209.11107*, 2022.

[8] F. Milano, B. Alhanjari, and G. Tzounas, "Enhancing frequency control through rate of change of voltage feedback," *IEEE Transactions on Power Systems*, pp. 1–4, 2023.

[9] X. He, V. Häberle, and F. Dörfler, "Complex-frequency synchronization of converter-based power systems," *arXiv*, vol. 2208.13860, 2022.

[10] D. Moutevelis, J. Roldán-Pérez, M. Prodanovic, and F. Milano, "Design of virtual impedance control loop using the complex frequency approach," in *2023 IEEE Belgrade PowerTech*, 2023, pp. 1–6.

[11] A. Büttner and F. Hellmann, "Complex couplings – A universal, adaptive and bilinear formulation of power grid dynamics," *arXiv*, no. 2308.15285, 2023.

[12] R. Teodorescu, M. Liserre, and P. Rodríguez, *Grid Synchronization in Three-Phase Power Converters*. John Wiley & Sons, Ltd, 2011, ch. 8, pp. 169–204, in *Grid Converters for Photovoltaic and Wind Power Systems*.

[13] Á. Ortega and F. Milano, "Comparison of different pll implementations for frequency estimation and control," in *2018 18th International Conference on Harmonics and Quality of Power (ICHQP)*, 2018, pp. 1–6.

[14] J. Nutaro and V. Protopopescu, "Calculating frequency at loads in simulations of electro-mechanical transients," *IEEE Transactions on Smart Grid*, vol. 3, no. 1, pp. 233–240, 2012.

[15] F. Milano and Á. Ortega, "Frequency divider," *IEEE Transactions on Power Systems*, vol. 32, no. 2, pp. 1493–1501, 2017.

[16] B. Tan, J. Zhao, F. Milano, Q. Lai, Y. Zhang, and D. A. Maldonado, "Extended frequency divider for bus frequency estimation considering virtual inertia from dfigs," in *IEEE ISGT Latin America*, 2021, pp. 1–5.

[17] M. Aghahassani, E. D. Castronuovo, P. Ledesma, and F. Milano, "Extended frequency divider formula with inclusion of DER control dynamics," in *IEEE PES General Meeting, Orlando*, 2023.

[18] I. Ponce and F. Milano, "Modeling hybrid ac/dc power systems with the complex frequency concept," *IEEE Transactions on Power Systems*, pp. 1–11, 2023.

[19] P. Sauer and M. Pai, *Power System Dynamics and Stability*. Prentice Hall, 1998.

[20] A. Yazdani and R. Iravani, *Voltage-sourced converters in power systems: modeling, control, and applications*. John Wiley & Sons, 2010.

[21] F. Milano, "A Python-based software tool for power system analysis," in *IEEE PES General Meeting*. IEEE, 2013, pp. 1–5.